JOURNAL OF SOLID STATE CHEMISTRY **124,** 292–299 (1996)
ARTICLE NO. 0239

Structural Phase Transitions and Pseudomerohedrally Twinning of Li_2FeBr_4

M. Partik,* Ch. Wickel,* H. D. Lutz,*,[1] and T. Roisnel†

*Anorganische Chemie I, Universität Siegen, D-57068 Siegen, Germany; and †Laboratoire Léon Brillouin, CEA-CNRS-Saclay F-91191 Gif-Sur-Yvette Cedex, France

Received November 13, 1995; in revised form April 4, 1996; accepted April 10, 1996

DEDICATED TO PROFESSOR MARIANNE BAUDLER ON THE OCCASION OF HER 75TH BIRTHDAY

The crystal structure of the quenched high-temperature phase Li_2FeBr_4, which is stable between 668 and 749 K, was determined by X-ray diffraction of a powdered sample and a twinned crystal (space group *Cmmm*, $Z = 2$, $a = 773.50(8)$, $b = 1093.6(1)$, $c = 382.58(4)$ pm, $R_I = 5.9\%$, $R(F) = 3.2\%$, 185 unique reflections, respectively). The six twin individuals are connected by one threefold rotation axis and, in addition, by three twofold rotation axes. Raman spectra and the ionic conductivity revealed Li_2FeBr_4 to be very similar to the orthorhombic low-temperature forms of Li_2MBr_4 (M = Mg, Mn). High-temperature X-ray and neutron diffraction experiments of quenched powder samples show the formation of an inverse spinel-type polymorph (space group $Fd\bar{3}m$, $Z = 8$, $a = 1115.2(1)$ pm, $R_I = 10.1\%$, $R_{wp} = 14.5\%$ at 660 K) in the temperature range 441–668 K.

INTRODUCTION

The isostructural, polymorphic ternary lithium bromides Li_2MgBr_4 and Li_2MnBr_4 (1) have been found to be fast lithium ion conductors. The room-temperature modifications of both compounds crystallize in an ordered orthorhombic NaCl defect structure (2, 3) (Mn_2SnS_4 type (4)). The two high-temperature polymorphs adopt a modified Zr_3S_4 structure (5) (space group $Fd\bar{3}m$, $Z = 8$), i.e., the so called Li_2MnBr_4 HTM I structure (6), and a disordered deficient NaCl structure (space group $Fm\bar{3}m$, $Z = 1$), respectively. An analogous compound Li_2FeBr_4 has not yet been reported, but Schmidt (7) observed the formation of a high-temperature phase Li_2FeBr_4 by thermoanalytical (DTA) measurements. We investigated this ternary high-temperature bromide, which can be quenched to ambient temperature, by X-ray powder and crystal diffraction as well as by Raman spectroscopic methods. In order to analyze structural phase transitions, we additionally performed high-temperature X-ray and neutron powder diffraction studies and impedance spectroscopic and thermoanalytical measurements.

EXPERIMENTAL

Polycrystalline samples of Li_2FeBr_4 were prepared by fusing stoichiometric amounts of anhydrous LiBr and $FeBr_2$ in evacuated quartz glass ampoules, annealing at 723 K for 5 days, and quenching to room temperature. LiBr was dried at 600 K in a vacuum. $FeBr_2$ was prepared by direct combination of the elements (8). Crystals of the high-temperature polymorph were obtained by slowly cooling down a molten sample from 773 to 733 K and quenching it to room temperature.

For the high-temperature X-ray studies, the Guinier powder technique, with an Enraf–Nonius Guinier-Simon FR 553 camera, was used. X-ray precession photographs of the crystal were taken with a Buerger precession camera using Mo$K\alpha$ radiation. Thermoanalytical measurements (differential scanning calorimetry, DSC) were performed on a Perkin–Elmer DSC 7 thermoanalyzer with heating rates of 20 K/min. Gold pans were used as sample holders.

X-ray powder diffraction intensities were measured with a Seifert powder diffractometer MZ4 with Cu$K\alpha$ radiation. The intensities of the crystals were collected on an Enraf–Nonius CAD4 diffractometer with graphit-monochromatized Mo$K\alpha$ radiation. The data set was taken over one hemisphere of the small orthorhombic cell (see below) in two different azimuth positions ($\psi = 0°$ and 90°) and with positive and negative Θ angles. All reflections were corrected for Lorentz and polarization effects. Empirical correction for absorption was made by ψ scans in a special manner (see below). For data reduction and absorption correction, the program NRCVAX (9) was used. The neutron diffraction data were collected on the high-resolution powder diffractometer 3T2 at the Laboratoire Léon Brillouin in Saclay (France). The neutron wavelength used

[1] To whom correspondence should be addressed.

0022-4596/96 $18.00

was 122.72 pm. The neutron scattering lengths were $b(Li) = -2.03$ fm, $b(Fe) = 9.45$ fm, and $b(Br) = 6.78$ fm. The structure refinements were performed with the programs DBWS-9006 (10) (X-ray powder data), PROFIL (11) (neutron powder data), and SHELXL-93 (12) (crystal data).

Raman spectra were performed with a Dilor Omars 89 multichannel Raman spectrograph using the 647.1 nm radiation of a Kr^+ laser for excitation. The impedance diagrams were determined with a Hewlett–Packard 4192A LF impedance analyzer. Details of the cell and the setup employed are given in (13).

RESULTS

1. High-Temperature X-ray and Thermoanalytical Measurements

High-temperature X-ray diffraction photographs of stoichiometric amounts of the binary bromides display the formation of an orthorhombic high-temperature phase Li_2FeBr_4 *oC*14 (Pearson symbol) (Fig. 1). On the DSC thermograms, two endothermic peaks are visible (Fig. 2). The first at 668(1) K (onset) is associated with the formation of the orthorhombic high-temperature phase; the second at 749(3) K is due to melting of the solid. High-temperature X-ray patterns and DSC diagrams of the quenched phase show an exothermic phase transition to a cubic modification (Li_2FeBr_4*cF*56) at 441 K, which can likewise be quenched to ambient temperature, and the endothermic rebuilding of the orthorhombic phase at 672 K (onset) (Figs. 3 and 4).

2. Raman Spectra

The Raman spectra (Fig. 5) display evident similarities among the orthorhombic high-temperature phase of Li_2FeBr_4 and the low-temperature modification of Li_2MnBr_4 (2) (see Table 1). Unit-cell group analysis on the basis of the space group *Cmmm* predicts (2) $\Gamma = 2\ A_g + 1\ A_u + 2\ B_{1g} + 3\ B_{1u} + 1\ B_{2g} + 4\ B_{2u} + 1\ B_{3g} + 4\ B_{3u}$. For Li_2FeBr_4 all six Raman-allowed modes are observed in the spectral region from 150 to 25 cm^{-1}. Substitution of manganese by iron results in strong shifts of the modes below 80 cm^{-1}. The wavenumbers of the two bands in the spectral region 150–125 cm^{-1} are approximately the same for both compounds as well as for Suzuki-type $Li_6M^{II}Br_8$ (M = Mn, Fe (2, 14)) (Table 1).

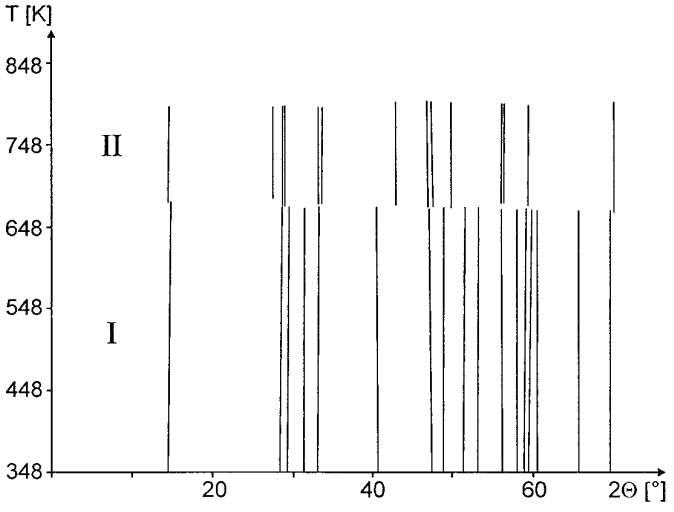

FIG. 1. High-temperature X-ray diffraction pattern ($CuK\alpha_1$) of stoichiometric amounts of the binary bromides LiBr and $FeBr_2$, I; Li_2FeBr_4 *oC*14, II.

3. Ionic Conductivity

The formation of the orthorhombic high-temperature modification is revealed by an increase of the electric conductivity and a decrease of the activation energy for conduction at 668 K (Fig. 6). The ionic conductivity of Li_2FeBr_4 is somewhat smaller than that of Li_2MBr_4 (M = Mn, Mg) (17, 18). The activation energy of conduction of a stoichiometric mixture of LiBr and $FeBr_2$ is much lower than that of LiBr and $CdBr_2$ (18). The activation energy of orthorhombic Li_2FeBr_4 (above 668 K) resembles that of Li_2CdBr_4 in the temperature range 518–628 K (18).

4. Powder and Crystal X-ray Refinements

X-ray precession photographs of the obtained crystals correspond to the orthorhombic space group *Immm* with an approximately tetragonal metric ($a \approx b \approx 770.0$ pm,

TABLE 1
Raman modes (cm^{-1}) of Mn_2SnS_4-type $Li_2M^{II}Br_4$ and Suzuki-type $Li_6M^{II}Br_8$ (M = Fe, Mn) (Assignment in Analogy to Those Given in (15, 16))

Species	$A_g(1)/A_{1g}$	$A_g(2)/E_g$	$B_{1g}(1)/F_{2g}(1)$	$B_{1g}(2)/F_{2g}(2)$	B_{2g}/B_{3g}
Li_2MnBr_4 (2)	145	126	98	66	38,81
Li_2FeBr_4	145	130	96	74	48,57
Li_6MnBr_8 (2)	144	125	74	64	—
Li_6FeBr_8 (14)	146	128	90	67	—

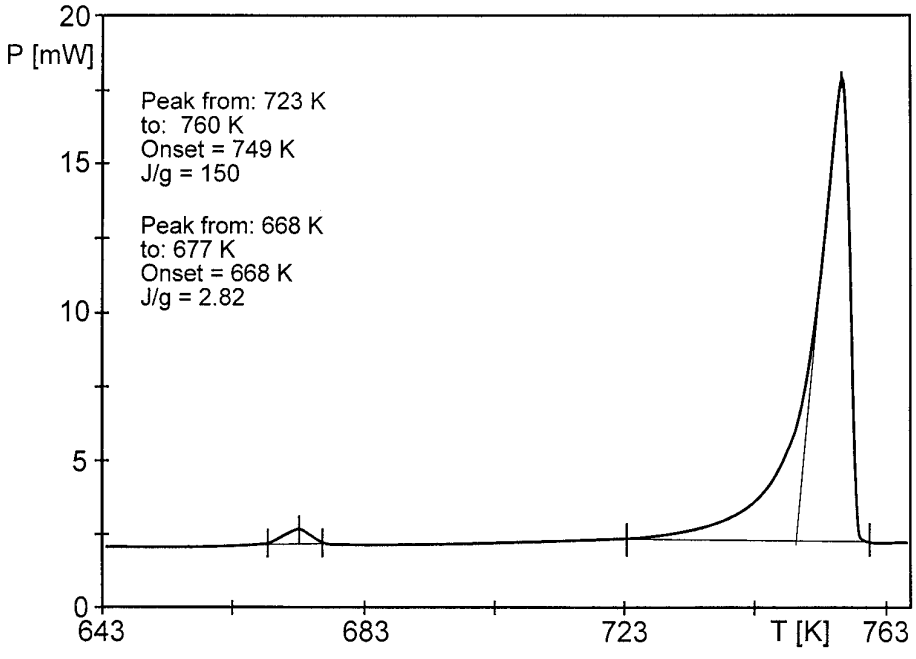

FIG. 2. DSC diagram of stoichiometric amounts of LiBr and $FeBr_2$.

c = 1093.6 pm), but none of the superstructure reflections in addition to those of the Mn_2SnS_4-type structure were found in the powder experiment. The X-ray powder data could be refined in the small orthorhombic cell (R_I = 5.9%) as shown in Tables 2 and 4. The observed and fitted diffraction patterns are shown in Fig. 7. Hence, we assume the formation of a multiple twin as in the case of Li_2CoCl_4 (19). The pattern on the X-ray precession photographs can be described as due to a superimposition of six individuals with the small orthorhombic cell (Fig. 8). The *hkl* indices for two of the three components are generated by using the matrix

$$(h\,k\,l)_{III} = (h\,k\,l)_I * \begin{pmatrix} 1\bar{2} & \bar{1} & 1\bar{4} \\ 1/2 & 0 & 1\bar{4} \\ 1 & \bar{2} & 1/2 \end{pmatrix} \qquad [1]$$

(for details see (19)) and, in addition, for the twinning by application of the matrix

$$(h\,k\,l)_{II} = (h\,k\,l)_I * \begin{pmatrix} 0 & 0 & 1/2 \\ 0 & \bar{1} & 0 \\ 2 & 0 & 0 \end{pmatrix} \qquad [2]$$

TABLE 2
Parameters of Data Collection and Rietveld Refinement of Li_2FeBr_4 *oC*14 (X-ray Powder Study)

2Θ range (°)	20–90
Step width (°)	0.02
T(K)	293
Space group	*Cmmm* (No. 65)
Lattice constants (pm)[a]	a = 773.31(5)
	b = 1093.43(7)
	c = 382.39(3)
	Z = 2
Parameters refined	15
Halfwidth parameters (°²)	
U	−0.16(5)
V	0.39(4)
W	−0.060(7)
Agreement factors	R_I = 5.9%
	R_{wp} = 8.2%
	R_{exp} = 10.6%

[a] As refined.

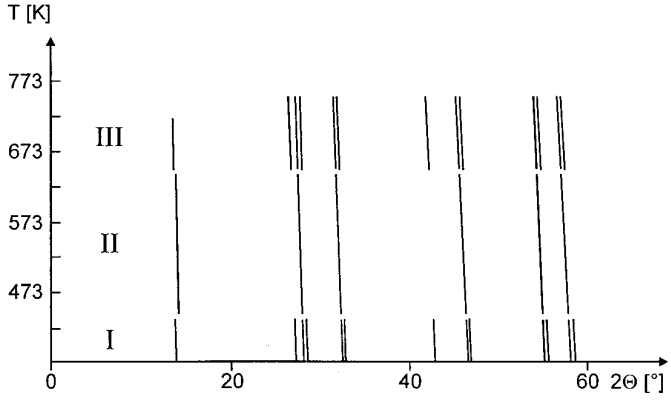

FIG. 3. High-temperature X-ray diffraction pattern (Cu$K\alpha_1$) of Li_2FeBr_4 *oC*14 (I and III); Li_2FeBr_4 *cF*56, II.

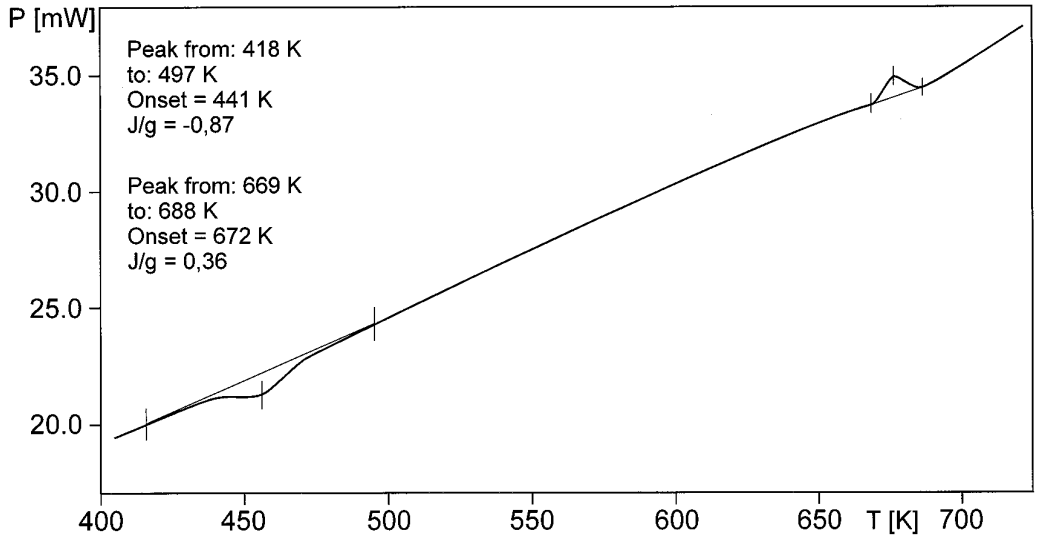

FIG. 4. DSC diagram of Li_2FeBr_4 *oC*14.

taken from (20). The absorption correction for the twin crystal was made by an intensity- and ratio-weighted method discussed in (21).

The experimental data and agreement factors ($R(F) = \Sigma|\ |F_0| - |F_c|\ |/\Sigma|F_0|$ and $wR^2 = (\Sigma[w(F_0^2 - F_c^2)^2]/\Sigma[wF_0^4])^2$) for the various refinements are shown in Table 3. The final atomic coordinates, and the isotropic and anisotropic thermal parameters of orthorhombic Li_2FeBr_4, which result by a refinement as multiple twin and a twin absorption correction, are given Table 4, selected distances and angles in Table 5. Representations of the $LiBr_6$ octahedra with anisotropic thermal parameters taken from refinement as twin by 120° rotation and as multiple twin with and without twin absorption correction are shown in Fig. 9. The results of the various refinements of the crystal experiment are given in Table 6.

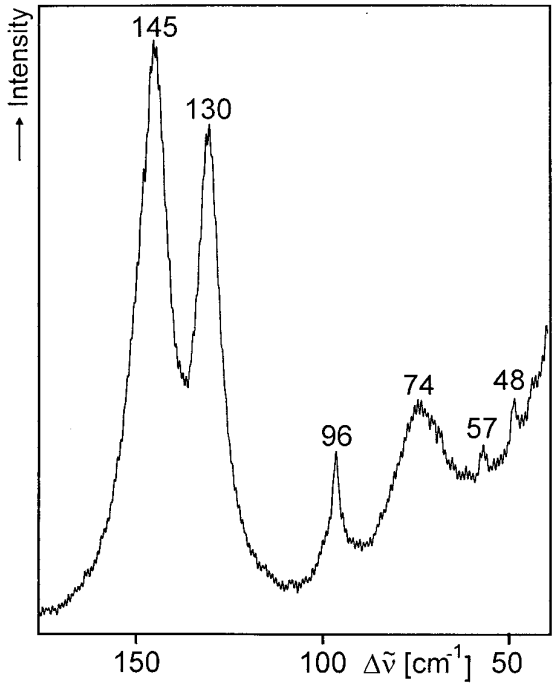

FIG. 5. Raman spectrum of Li_2FeBr_4 *oC*14.

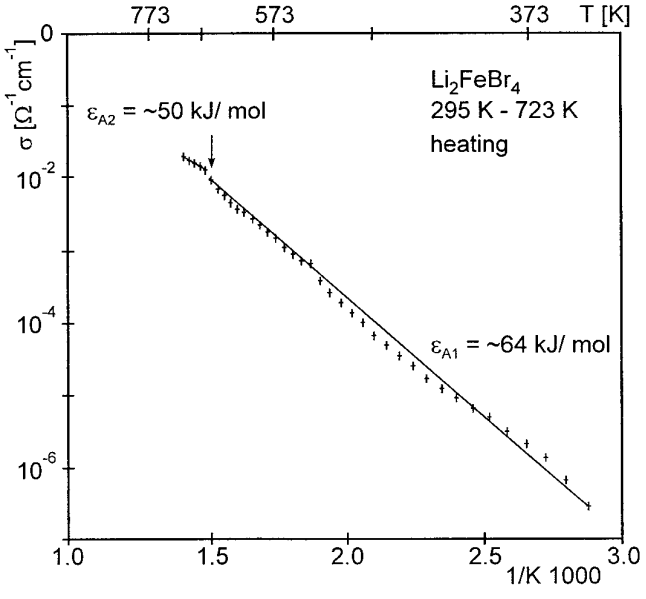

FIG. 6. Arrhenius plot of the electric conductivity of stoichiometric amounts of LiBr and $FeBr_2$ (heating curve; arrow, formation of Li_2FeBr_4; ε_A, activation energy of conduction).

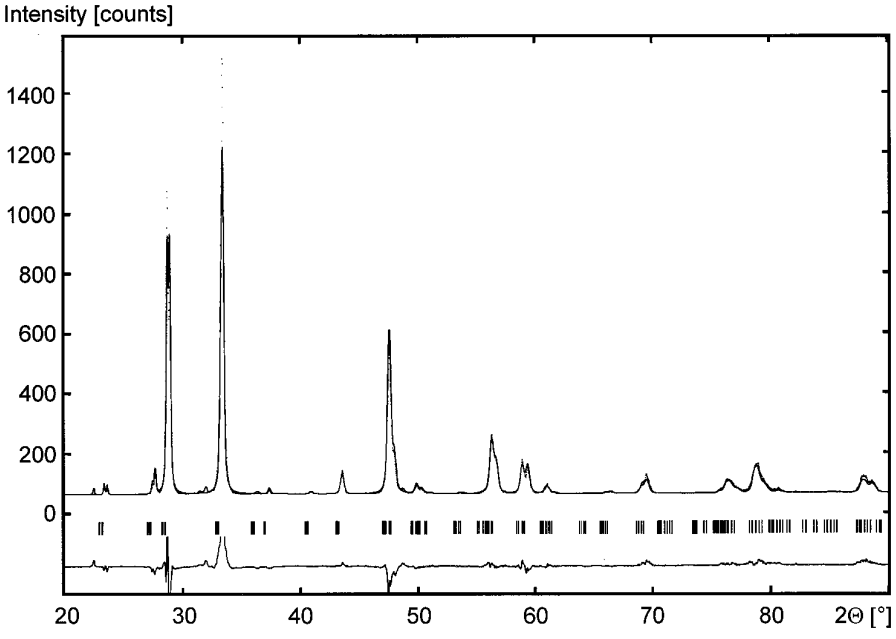

FIG. 7. Observed (···), fitted (—), and difference X-ray diffraction profiles of quenched orthorhombic Li_2FeBr_4. Calculated 2Θ values are marked by vertical bars (|).

TABLE 3
Parameters Used for Data Collection and *R* Values of the Twinned Trilling Crystal Refinement of Li_2FeBr_4 *oC*14

Color	brown–yellow
Space group	*Cmmm* (No. 65)
Lattice constants (pm)[a]	a = 773.5(1) b = 1093.60(8) c = 382.6(1)
Unit-cell volume (pm^3)	323.6(1) × 10^6 Z = 2
Calculated density (g/cm^3)	3.996
Crystal dimensions (mm^3)	0.21 × 0.19 × 0.20
Twin volume ratios	0.00(1) : 0.51(1) : 0.12(1) : 0.16(1) : 0.04(1) : 0.18(1)
T (K)	293
Scan mode	ω
h, k, l ranges	$-9 \le h \le 9$; $-12 \le k \le 12$; $-4 \le I \le 4$
No. of reflections measured	6707
No. of reflections refined	1955
No. of reflections observed ($>2\sigma_I$)	1694
No. of unique reflections	185
Parameters refined	22
Linear absorption coefficient (cm^{-1})	26.88
Extinction coefficient (12)	0.0(4) × 10^{-4}
Agreement factors	
$R(F)$ all	6.7%
$R(F)$ obs.	5.9%
wR^2 obs.[b]	12.2%
$R(F)$ after merging	3.2%

[a] Obtained from Guinier photographs.

[b] Weighting scheme: $w = 1/[\sigma^2 (F_0)^2 + (0.00 \times P)^2 + 5.0 \times P)$; $P = (F_0^2 + F_c^2)/3$.

5. Neutron Powder Diffraction

Neutron powder diffraction measurements were performed of quenched Li_2FeBr_4 at 660 K. The refinements with the modified Rietveld program PROFIL (11) revealed that this high temperature modification crystallizes in an inverse spinel structure with partial disordering of the lith-

TABLE 4
Final Atomic Coordinates and Displacement Parameters ($U_{ij}/10^4$ pm^2) of Li_2FeBr_4 *oC*14 Obtained by the Twin Refinement with a Multiple Twin Absorption Correction (21)

Atom	Site	x	y	z	$U_{eq}/[U_{iso}]$
Fe	2*a*	0.0	0.0	0.0	0.0156(5)
		[0.0	0.0	0.0	0.039(1)]
Li	4*f*	0.25	0.25	0.5	0.052(6)
		[0.25	0.25	0.5	0.041(1)[a]]
Br(1)	4*h*	0.2366(2)	0.0	0.5	0.0146(3)
		[0.2373(5)	0.0	0.5	0.042(1)]
Br(2)	4*i*	0.0	0.2420(1)	0.0	0.0156(3)
		[0.0	0.2427(4)	0.0	0.044(1)]

	U_{11}	U_{22}	U_{33}	U_{23}	U_{13}	U_{12}
Fe	0.019(2)	0.013(2)	0.015(1)	0.0	0.0	0.0
Li	0.06(2)	0.03(2)	0.06(2)	0.0	0.0	−0.03(1)
Br(1)	0.0156(7)	0.0090(8)	0.0192(7)	0.0	0.0	0.0
Br(2)	0.0201(8)	0.0085(8)	0.0182(7)	0.0	0.0	0.0

Note. U_{eq} is defined as $T = \exp(-8\pi^2 U (\sin^2 \Theta)/\lambda^2)$ and U_{ij} as $T = \exp(-2\pi^2 \Sigma_i \Sigma_j U_{ij} h_i h_j a_i^* a_j^*)$. The powder data are given in square brackets.

[a] Overall temperature factor.

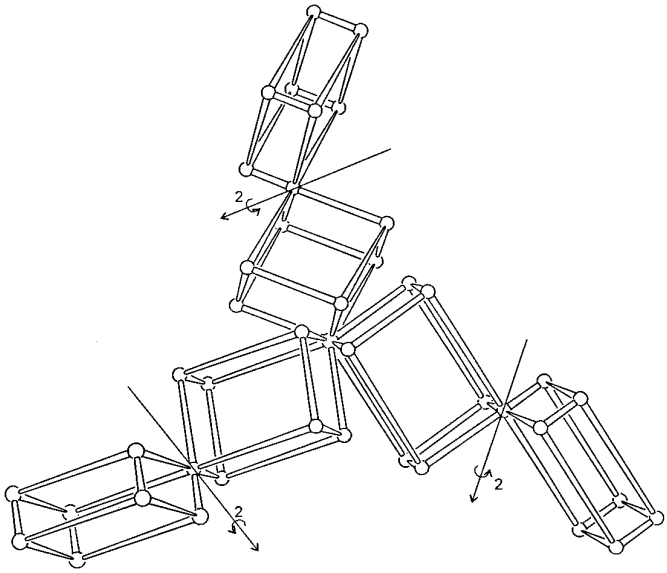

FIG. 8. Orientation of the six individuals of the twinned trilling.

TABLE 5

Selected Distances (pm) and Angles (°) of Li_2FeBr_4 *oC*14 (Calculated from Fractional Coordinates of the Twin Refinement (Table 4) and the Unit-Cell Dimensions Computed from Guinier Photographs (Table 3))

	$FeBr_6$ octahedron		
4 × Fe–Br(1)	264.7(1)	2 × Br(1)–Fe–Br(1)	92.53(5)
2 × Fe–Br(2)	264.7(2)	2 × Br(1)–Fe–Br(1)	87.47(5)
		1 × Br(2)–Fe–Br(2)	180.0
		8 × Br(1)–Fe–Br(2)	90.0
	$LiBr_6$ octahedron		
2 × Li–Br(1)	273.60(2)	1 × Br(1)–Li–Br(1)	180.0
4 × Li–Br(2)	272.14(4)	4 × Br(1)–Li–Br(2)	86.62(4)
		4 × Br(1)–Li–Br(2)	93.38(4)
		2 × Br(2)–Li–Br(2)	89.32(2)
		2 × Br(2)–Li–Br(2)	90.68(2)
		2 × Br(2)–Li–Br(2)	180.0

ium ions from the tetrahedral 8*a* site to the interstitial octahedral 16*c* site as found in the related compound Li_2FeCl_4 (22). The diffraction pattern obtained at 660 K is shown in Fig. 10. The structure was refined in space group $Fd\bar{3}m$. The final R values are $R_{wp} = 14.5\%$, $R_{exp} = 6.8\%$, and $R_I = 10.1\%$. The profile and structural parameters are given in Table 7, the bond lengths and angles, which were calculated with the lattice constant of the Rietveld refinement, in Table 8. To our knowledge, Li_2FeBr_4 is the first bromide with tetrahedrally coordinated lithium ions known so far.

DISCUSSION

The orthorhombic high-temperature phase of Li_2FeBr_4 adopts a Mn_2SnS_4-type structure (4). It is the thermodynamically stable polymorph in the range from 668 to 749 K. Below this temperature, the binary bromides or $FeBr_2$ and Suzuki-type Li_6FeBr_8 (14) are thermodynamically preferred. Li_2FeBr_4 can be obtained in a cubic modification by annealing the quenched orthorhombic phase above 441 K. This modification is thermodynamically less stable than the mixture of the origin components LiBr and $FeBr_2$, but it is stabler than orthorhombic Li_2FeBr_4 at $T < 668$ K. Both polymorphes can be quenched to room-temperature because their decomposition is kinetically hindered.

The reason of the existence of spinel-type Li_2FeBr_4 below 668 K, in contrast to the behavior of Li_2MnBr_4 and Li_2MgBr_4 (1, 6), may be the shorter Li–Br distances possible in the tetrahedral voids compared to those of the latter compounds. Thus, some additional bonding energy due to the more covalent nature of $LiBr_4$ units (14) compared to $LiBr_6$ units can occur irrespective of the more favored binary bromides in that temperature range. The disorder

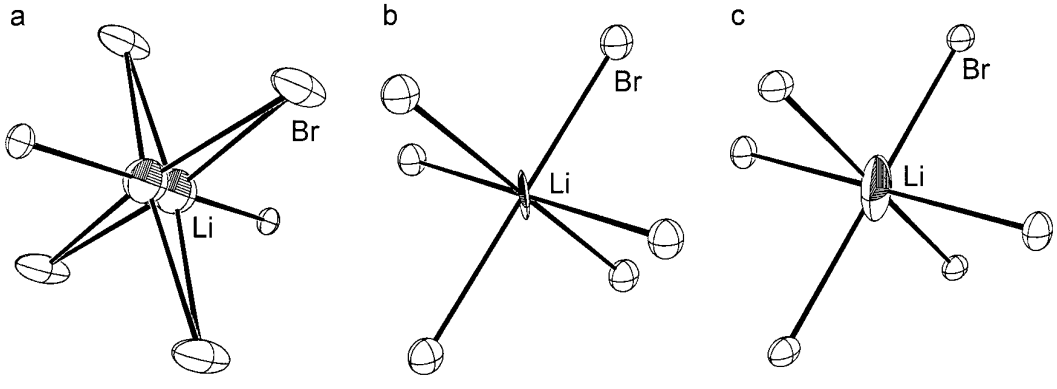

FIG. 9. Illustration of the anisotropic thermal parameters of the $LiBr_6$ octahedra of Li_2FeBr_4 *oC*14. (Refinement as trilling with split position of the lithium (a), as twinned trilling with overall absorption correction (b), and twinned trilling with 'trilling' absorption correction (c).)

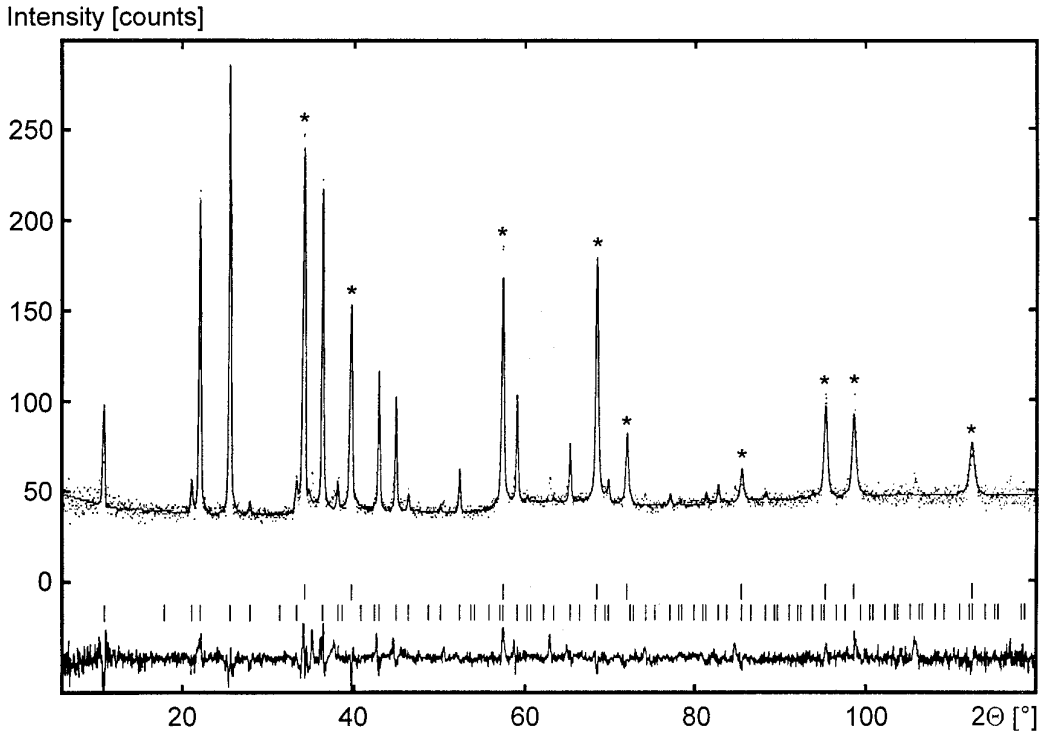

FIG. 10. Observed (···), fitted (—), and difference neutron diffraction profiles of cubic Li_2FeBr_4 at 670 K. Calculates 2Θ values are marked by vertical bars (|). * denote reflections caused by the sample holder (copper).

of the tetrahedrally coordinated lithium ions to the interstitial 16*c* sites resembles that of the spinel-type chlorides (23).

The structural phase transition of Li_2FeBr_4 *oC*14 at temperatures above 668 K to a cubic modification (Li_2MnBr_4 HTM I type) in analogy to the behavior of other ternary lithium bromides was not observed. Thus, the twinning is not the result of a transition by symmetry reduction as in the case of Li_2CoCl_4, but probably an effect of crystal growth. On the other hand, formation of a disordered deficient NaCl-type phase in a small temperature range below the melting point cannot be excluded. In this case, symmetry reduction by two lattice equivalent transformations in analogy to that of Li_2CoCl_4 causes the pseudomerohedral twinning. The first-order transformation from space group $Fd\bar{3}m$ to *Cmmm*, as pointed out in (19, 20), however, is not expected because a Li_2MnBr_4 HTM I-type phase was not observed. In this case, two different sequences for the lattice equivalent phase transitions are possible. First, a lattice equivalent transition of index 2, which describes the merohedral twinning from a structure with Laue symmetry $m\bar{3}m$ to one with the Laue symmetry $m\bar{3}$ and subsequently the pseudomerohedral formation of the twin by 120° rotation. Second, symmetry reduction with index 3 from cubic to tetragonal holohedry and subsequently a pseudomerohedral transformation by losing the fourfold rotation axis. The twinning by 180° rotation is probably the result of ordering of the lithium atoms. This is shown from the splitting of the lithium position by the refinement as twin by 120° rotation.

TABLE 6
Agreement Factors of the Various Refinements of the Crystal Data of Li_2FeBr_4 *oC*14

Refinement condition	Multiple twinned crystal[a] (%)	Twin crystal by 120° rotation (%)	Twin crystal by 180° rotation (%)	Single crystal small o-rh. cell (%)
$R(F)$ all	6.9	7.6	8.4	8.8
$R(F)$ after merging	3.3	4.4	7.1	7.7

[a] Overall empirical absorption correction.

TABLE 7
Parameters of Data Collection and Rietveld Refinement of Li_2FeBr_4 *cF*56 (Neutron Powder Study)

2Θ range (°)	6–120
Step width (°)	0.05
T (K)	670
Space group	$Fd\bar{3}m$ (No. 227)
Lattice constant (pm)[a]	1115.2(1)
	$Z = 8$
Parameters refined	13
Halfwidth parameters (°²)	
U	0.2(1)
V	−0.19(8)
W	0.10(1)
Agreement factors	$R_I = 10.1\%$
	$R_{wp} = 14.5\%$
	$R_{exp} = 6.8\%$

Atom	Site	Occupation	x	y	z	$B_{iso}/10^4$ pm²
Li(1)	8*a*	0.33(6)	0.125	0.125	0.125	5.5(2)
Li(2)	16*c*	0.34(3)	0	0	0	17(7)
Li(3)	16*d*	0.5	0.5	0.5	0.5	5.9(5)
Fe	16*d*	0.5	0.5	0.5	0.5	5.9(5)
Br	32*e*	1.0	0.2531(7)	0.2531(7)	0.2531(7)	5.5(2)

Note. B_{iso} is defined as $T = \exp(-B\ (\sin^2 \Theta)/\lambda^2)$.
[a] As refined.

TABLE 8
Selected Distance, (pm) and Angles (°) of Li_2FeBr_4 *cF* 56

	$Fe/Li(3)Br_6$ octahedron		
6 × Fe/Li(3)–Br	282.3(8)	6 × Br–Fe/Li(3)–Br	88.6(2)
6 × Br–Br	384(1)	6 × Br–Fe/Li(3)–Br	91.4(2)
6 × Br–Br	395(1)	3 × Br–Fe/Li(3)–Br	180.0
	$Li(2)Br_6$ octahedron		
6 × Li(2)–Br	282.3(8)	6 × Br–Li(2)–Br	88.6(2)
6 × Br–Br	384(1)	6 × Br–Li(2)–Br	91.4(4)
6 × Br–Br	395(1)	6 × Br–Li(2)–Br	180.0
	$Li(1)Br_4$ tetrahedron		
4 × Li(1)–Br	247.4(8)	6 × Br–Li(1)–Br	109.5
6 × Br–Br	404(1)		

ACKNOWLEDGMENTS

The authors thank the Graduiertenkolleg ''Chemische Reaktivität und molekulare Ordnung'' of the University of Siegen, the Deutsche Forschungsgemeinschaft, and the Fonds der Chemischen Industrie for financial support.

REFERENCES

1. M. Schneider, P. Kuske, and H. D. Lutz, *Thermochim. Acta* **215,** 219 (1993).
2. H. D. Lutz, M. Schneider, P. Kuske, and H. J. Steiner, *Z. Anorg. Allg. Chem.* **592,** 106 (1991).
3. M. Schneider, P. Kuske, and H. D. Lutz, *Z. Naturforsch. B* **48,** 1 (1993).
4. M. Partik, Th. Stingl, H. D. Lutz, H. Sabrowsky, and P. Vogt, *Z. Anorg. Allg. Chem.* **621,** 1600 (1995).
5. H. Hahn, B. Harder, U. Mutschke, and P. Ness, *Z. Anorg. Allg. Chem.* **292,** 82 (1957).
6. H. D. Lutz, J. K. Cockcroft, P. Kuske, and M. Schneider, *Mater. Res. Bull.* **25,** 451 (1990).
7. W. Schmidt, Doctoral Thesis, University of Siegen, 1983.
8. F. Schimmel, *Chem. Ber.* **62,** 963 (1929).
9. E. J. Gabe, Y. LePage, J.-P. Charland, F. L. Lee, and P. S. White, *J. Appl. Crystallogr.* **22,** 384 (1989).
10. A. Sakthivel and R. A. Young, School of Physics, Georgia Institute of Technology, Atlanta, Ga 300332 USA (1990).
11. J. K. Cockcroft, ''PROFIL, Version 5.17.'' Institute Laue-Langevin, Grenoble, France, 1994.
12. G. M. Sheldrick, ''SHELXL-93, Program for Crystal Structure Refinement.'' Univ. Göttingen, 1993.
13. H. D. Lutz, A. Pfitzner, and Ch. Wickel, *Solid State Ionics* **48,** 131 (1991).
14. M. Partik, Doctoral Thesis, University of Siegen (1996).
15. H. C. Gupta, J. Zwinscher, and H. D. Lutz, *J. Phys. Chem. Solids,* in press.
16. J. Zwinscher, H. D. Lutz, and H. C. Gupta, *J. Solid State Chem.,* in press.
17. R. Kanno, Y. Takeda, O. Yamamoto, Ch. Cros, G. Wang, and P. Hagenmuller, *J. Electrochem. Soc.* **133,** 1052 (1986).
18. W. Schmidt and H. D. Lutz, *Ber. Bunsenges. Phys. Chem.* **88,** 720 (1984).
19. M. Schneider, H. D. Lutz, and J. K. Cockcroft, *Z. Kristallogr.* **203,** 183 (1993).
20. M. Schneider, Doctoral Thesis, University of Siegen (1991).
21. M. Partik, Ch. Kringe, and H. D. Lutz, *Z. Kristallogr.* **211,** 304 (1996).
22. H. D. Lutz. A. Pfitzner, and J. K. Cockcroft, *J. Solid State Chem.* **107,** 245 (1993).
23. H. J. Steiner and H. D. Lutz, *J. Solid State Chem.* **99,** 1 (1992).